Observation of Large Kerr Angles in the Nonlinear Optical Response from Magnetic Multilayers

Bert Koopmans, Marcel Groot Koerkamp, and Theo Rasing
Research Institute for Materials, Toernooiveld, 6525 ED Nijmegen, The Netherlands

Hugo van den Berg
Siemens AG, D-91052 Erlangen, Germany
(Received 20 October 1994)

We have observed a longitudinal nonlinear (second-harmonic) Kerr rotation up to 22° for an Fe(2 nm)/Cr(2 nm) multilayer on an SiO_2 substrate that shows a linear Kerr rotation of only a few hundreths of a degree. The latter value excludes any linearly induced mechanism and confirms the interface sensitivity of this nonlinear Kerr technique. The enormous enhancement is shown to be in good agreement with recent predictions, based on spin dependent band structure calculations. The local optical field effects are shown to play an important role for the additional enhancements for such multilayers on a substrate.

PACS numbers: 75.70.Cn, 42.65.Ky, 78.66.−w

The magnetism of surfaces, thin films, and multilayers has recently attracted a great deal of interest [1]. The manipulation of artificial structures down to the atomic level has led to some surprising new results, such as the change of magnetization direction from normal to in plane for thin Fe films [2], enhanced or reduced magnetic moments at surfaces [1,3], and the oscillating exchange coupling through nonmagnetic spacers [5–8]. Besides their fundamental interest, these systems are also interesting for their potential in practical applications.

One of the most widely used techniques to study the magnetic properties of magnetic thin films is the magneto-optical Kerr effect (MOKE). In addition, MOKE is widely used for magnetic imaging. In this context, and also to study very thin films, large Kerr rotation angles are favorable.

Recently, it has been pointed out by Pustogowa, Hübner, and Bennemann that in nonlinear optical second-harmonic generation (SHG) from magnetic materials enormous enhancements of the Kerr angles can be expected [9]. This was indeed observed for the Heussler alloy PtMnSb [10], that is of course also known for its large linear Kerr rotation. However, more interesting applications of SHG can be found in the study of surfaces and interfaces of thin magnetic multilayers. Based on the symmetry breaking at interfaces, the second order nonlinear optical response is found to be extremely surface and interface sensitive [11]. Predictions of sensitivity for surface magnetism [12,13] were experimentally confirmed for clean surfaces [14,15] and multilayer interfaces [16,17] where relative magnetic effects in the SHG intensity of more than 50% have been observed. Despite the interesting theoretical studies on the nonlinear Kerr rotation angle $\phi_K^{(2)}$, to the best of our knowledge no attempts have been made so far to measure this quantity for a clean surface or a multilayer structure [18].

In this paper we present experimental nonlinear Kerr data for a magnetic Fe/Cr multilayer in the longitudinal configuration. We show that extremely large nonlinear Kerr angles are found for this very thin magnetic layer, for which the linear magneto-optical Kerr rotation is (vanishingly) small. Experimentally $\phi_K^{(2)}$ is found to be largest for the s-polarized input, with values between 5° and 22° for angles of incidence between 15° and 70°. For the p-input configuration we measure a rotation angle of 1° to 5° for incident angles between 15° and 70°. This is shown to be in good agreement with the results of band structure calculations on (bulk) Fe surfaces by Pustogowa, Hübner, and Bennemann [9]. We will also show how the substrate, through local field effects, can influence the magnitude of the observed $\phi_K^{(2)}$.

The sample consisted of a thin Fe film (thickness 2 nm), covered with a 2 nm Cr film deposited by rf diode and dc magnetron sputtering, respectively. As a substrate we used a (100) silicon wafer, with a thermal oxide layer of about 525 nm. The substrate was on a rotating table, which moved with a velocity of 0.96 and 3.97 m/min underneath the Fe and Cr targets, respectively. Both targets were equipped with screens for getting uniformity of the layer thickness better than 1%. The base pressure was 2×10^{-7} Torr and the Ar pressure was 5 mTorr. For the second harmonic experiments we used the 770 nm output of a mode-locked (80 MHz) Ti-sapphire laser. The pulse width was 70 fs and the input power was 100 mW focused on a spot diameter of 100 μm. The experiments were done in the longitudinal configuration, i.e., the magnetization $\boldsymbol{M}$ was in the plane of the sample and in the optical plane of incidence (see inset, Fig. 1).

Figure 1 shows the polarization dependence of the SH signal for an s-polarized input at an angle of incidence of 45° and for $\boldsymbol{M}$ along $\hat{x}$ and $-\hat{x}$, respectively. The difference between the two minima of the curves corresponds to

 0031-9007/95/74(18)/3692(4)$06.00

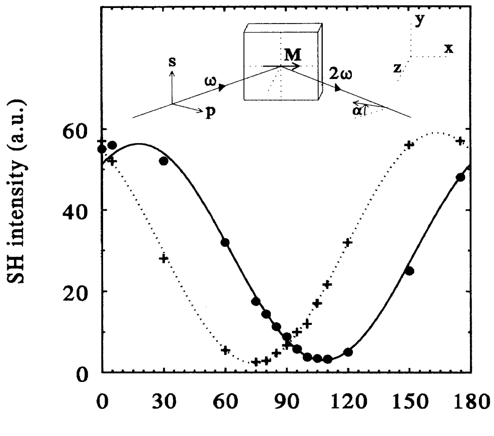

FIG. 1. Output polarization dependence of SHG reflection from an Fe/Cr multilayer, for s-polarized input. Filled dots: $\boldsymbol{M} \parallel \hat{x}$; crosses: $\boldsymbol{M} \parallel -\hat{x}$. The inset shows the experimental configuration.

$2\phi_K^{(2)} \approx 34°$, i.e., a nonlinear Kerr rotation $\phi_K^{(2)}$ of 17°. In this geometry we measured a linear Kerr angle of 0.03°, using the same Ti-sapphire input beam. These observations correspond to an enhancement of almost *3 orders* of magnitude for the nonlinear Kerr rotation. The small linear rotation can be compared with the bulk Fe value of 0.1°. The observed enormous enhancement is due to a combination of effects: The nonlinear $\phi_K^{(2)}$ is expected to be an order of magnitude larger than the linear counterpart and, contrary to the linear case, is also unaffected by the thickness reduction. The latter follows from the surface sensitivity of this nonlinear technique, as explained by the analysis below.

Following the approach of Pan, Wei, and Shen [12], it is convenient to separate the SH susceptibility into an even (χ^+) and an odd (χ^-) part in the magnetization $\boldsymbol{M}$. Thus, the induced SH polarization at an interface $\boldsymbol{P}(2\omega)$ is given by

$$P_i(2\omega) = \chi_{ijk}^+(\boldsymbol{M})E_jE_k + \chi_{ijk}^-(\boldsymbol{M})E_jE_k\,, \qquad (1)$$

where $\boldsymbol{E}$ is the local excitation field at frequency ω at the interface, and we implicitly assumed a summation over the repeated indices. The introduced susceptibilities fulfill $\chi_{ijk}^{\pm}(-\boldsymbol{M}) = \pm\chi_{ijk}^{\pm}(\boldsymbol{M})$. In the following we will drop the explicit $\boldsymbol{M}$ dependence of $\chi_{ijk}^{\pm}$. For a given surface symmetry the χ_{ijk}^+ and χ_{ijk}^- can be easily derived (see Table I). In the longitudinal configuration and for pure p- or s-input polarization we find that all nonzero χ_{ijk}^+ elements have $i \in \{x, z\}$, giving rise to p-polarized SHG. All nonzero χ_{ijk}^- elements have $i = y$, always resulting in s-polarized SHG. From this it follows that the SHG polarization ellipses for $\pm\boldsymbol{M}$ are each other's mirror image in the plane of incidence, and we can define a nonlinear Kerr angle $\phi_K^{(2)}$ in correspondence with its linear counterpart $\phi_K^{(1)}$.

TABLE I. The nonzero elements of the SH susceptibility tensor for an isotropic surface in the longitudinal configuration ($\boldsymbol{M} \parallel \hat{x}$). The two columns list the elements that are even and odd in the magnetization, respectively. The occurrence of the elements in the p- and s-input configurations is indicated within brackets.

χ^+		χ^-	
zxx	(p)	yxx	(p)
zyy	(s)	yyy	(s)
zzz	(p)	yzz	(p)
$xzx = xxz$	(p)	$zyz = zzy$	
$yzy = yyz$		$xyx = xxy$	

The nonlinear Kerr angle can be expressed in the s and p components of the reflected SH field, denoted by $E_s(2\omega)$ and $E_p(2\omega)$, respectively. Defining $R \equiv \mathrm{Re}[E_s(2\omega)/E_p(2\omega)]$, $I \equiv \mathrm{Im}[E_s(2\omega)/E_p(2\omega)]$, and $A^2 = R^2 + I^2$ we get

$$\phi_K^{(2)} = \tfrac{1}{2}\arctan[2R/(1 - A^2)] + \phi_0\,, \qquad (2)$$

with $\phi_0 = 0$ for $A^2 \leq 1$, $\phi_0 = 90°$ for $A^2 > 1$ and $R \geq 0$, and $\phi_0 = -90°$ for $A^2 > 1$ and $R < 0$. It is easily verified that in the limit $A \ll 1$ Eq. (2) reduces to $\phi_K^{(2)} = R$. However, the nonlinear case generally is far from this limit, since $\phi_K^{(2)}$ can become as large as 90°.

Inspection of Table I shows that the s-input configuration is particularly simple, with only one even χ_{zyy}^+ and one odd χ_{yyy}^- contributing element per interface. For normal incidence, only the χ_{yyy}^- contribution survives. From $E_p(2\omega) = 0$ we then find $\phi_K^{(2)} = \pm 90°$. Moving away from normal incidence, the ratio $|E_s(2\omega)/E_p(2\omega)|$, and as a consequence $|\phi_K^{(2)}|$, decreases so that $\phi_K^{(2)}$ is tunable over a wide range while scanning the angle of incidence.

A similar argument for a large $\phi_K^{(2)}$ close to normal incidence is found for a p-polarized input configuration. Table I shows that close to normal incidence the dominating even tensor components have one z index, and thus vanish at normal incidence, whereas the dominant odd tensor element, χ_{yxx}^-, is finite at normal incidence. (This seems in contradiction with Fig. 3 of Ref. [9]. However, there one has only considered χ_{yzz}^- that also vanishes at normal incidence.)

So far, we have only discussed the effects of the different tensor components. However, in an actual experiment, SHG intensities and polarizations are measured that are determined by both $\chi^{(2)}$ as well as the local fields. The latter can drastically alter the efficiency of different components (and, for instance, lead to very small intensities near normal incidence). Note that due to the very small linear Kerr angles a rotation of the local linear fields due to the linear Kerr effect can be neglected. For a multilayer structure, these local electric fields have recently been derived by Wierenga, Prins, and Rasing using a transfer matrix technique [19]. It can be shown that for the general case of an N-layer structure, the generated SH field can be written in the following form:

$$E(2\omega) = \frac{4\pi i\omega}{c\cos\theta}\sum_j [e_j(2\omega)\cdot \chi_j^{(2)} : e_j(\omega)e_j(\omega)], \quad (3)$$

where

$$e_{j,\mu}(\omega') = \frac{M_{j,N+1_\mu}^{++}(\omega') + M_{j,N+1_\mu}^{-+}(\omega')}{M_{0,N+1_\mu}^{++}(\omega')}\hat{e}_\mu(\omega'), \quad (4)$$

and we introduced the polarization vectors of the fundamental incident wave $\hat{e}(\omega)$ and reflected SH wave $\hat{e}(2\omega)$. The field amplitudes of the downward $(-)$ and upward $(+)$ propagating waves of frequency $\omega' = \omega$ or $\omega' = 2\omega$ at interface j are indicated by $E_j^{\pm}(\omega')$. $M_{j,j'\mu}^{++}(\omega')$ is the transfer matrix, relating the μ components of the fields at interfaces j and j'. ($j = 0$ and $j = N + 1$ indicate the outer surfaces on either side of the multilayer.)

Equations (3) and (4) become particularly attractive for contributions from the outer surface of the multilayer system ($j = 0$), for which Eq. (4) reduces to

$$e_{0,\mu}(\omega') = [1 + R_{0,N+1_\mu}(\omega')]\hat{e}_\mu(\omega'), \quad (5)$$

with $R_{0,N+1_\mu}(\omega)$ the total reflection coefficient of the system. $R_z = -R_x = R_p$, the p-polarization coefficient, and $R_y = R_s$, the s-polarization coefficient.

Figure 2 shows the observed nonlinear Kerr rotation for both s- and p-polarized input, as a function of the angle of incidence. We observed a small in-plane anisotropy in our experimental results, that is possibly induced by the sputtering process. The plotted data in Fig. 2 have been averaged over this azimuthal anisotropy. The solid curves in Fig. 2 are theoretical fits, with the unknown interface tensor elements of Table I as parameters and the following assumptions. Only the Fe is expected to contribute to the magnetic (odd) nonlinear susceptibility, because the Cr film is antiferromagnetic. Furthermore, the top Cr layer will be oxidized, so that the major contribution to the nonmagnetic nonlinear susceptibility is also expected to originate from the Fe film. Therefore we assigned effective SH susceptibilities to the Fe and Cr layers together. We verified that the actual position within the Cr/Fe top layer did not significantly change the results of our fits. In addition to these SH sources at the top layer, we incorporate a nonmagnetic SH source at the Si/oxide interface. The bulk optical constants were obtained from [20].

Because of the limited number of parameters involved in the s-polarization configuration (χ_{yyy}^- and χ_{zyy}^+ at the top layer, and χ_{zyy}^+ at the Si/oxide interface) one finds a unique fit to the experimental data points. The fit in Fig. 2 includes a relative maximum of $|\phi_K^{(2)}|$ near $\Theta_i \approx 65°$, that is due to an enhancement effect through multiple reflections in the thick silicon oxide layer. Similar, but smaller, enhancement factors due to a substrate are also known for the linear Kerr angle [21].

For the p polarization, several combinations of tensor elements give satisfying fits. Figure 2 gives one such solution, obtained by choosing fixed values for the relative phase factors and fitting the absolute values of the tensor components. At 45° angle of incidence, we experimentally find for the p input $\phi_K^{(2)} = 4.9°$.

From our thin film analysis, the expected nonlinear Kerr rotation of a semi-infinite bulk Fe crystal can be calculated in a straightforward way. Figure 3 shows the result of such a simulation for the s polarization. Preliminary experimental results on such a bulk surface show good agreement with this simulation [22]. Scaling our p-polarized result in the same way we find for the bulk nonlinear rotation $\phi_K^{(2)} = 2.4°$, in quite good agreement with the theoretical prediction for the surface of a bulk Fe crystal of Pustogowa, Hübner, and Bennemann [9]: $\phi_K^{(2)} = 1.4°$.

Figure 3 also includes the simulation for the same multilayer, but on a substrate with only a 10 nm SiO_2 layer. The different dependences and values for $\phi_K^{(2)}$ as a function of the angle of incidence demonstrate the importance of the multiple reflections and of the local field effects and thus the role of the substrate. Without

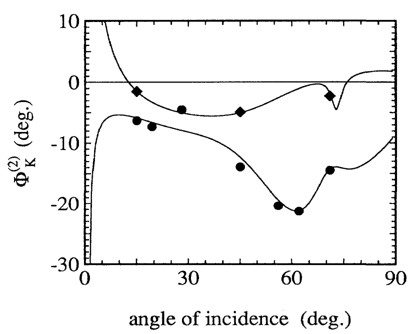

FIG. 2. Nonlinear Kerr rotation $\phi_K^{(2)}$ for an Fe/Cr multilayer as a function of the angle of incidence. Dots: s-input polarization; diamonds: p-input polarization. The curves are theoretical fits.

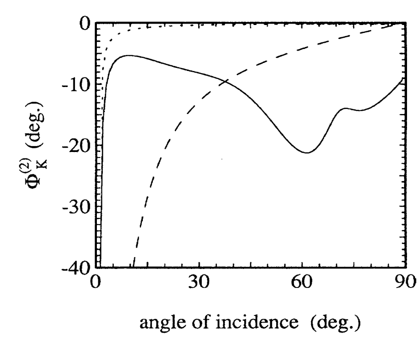

FIG. 3. Nonlinear Kerr rotation $\phi_K^{(2)}$ for an Fe/Cr multilayer and a bulk Fe surface for s-polarized input as a function of the angle of incidence. The bold solid line is the theoretical fit of Fig. 2. The dashed line is a simulation for $\phi_K^{(2)}$ of a clean Fe surface, based on the multilayer fit. The dotted line is a simulation for $\phi_K^{(2)}$ for an Fe/Cr multilayer on a silicon wafer with a 10 nm oxide.

going through a complete calculation, one can simply get an intuitive idea about this role. Let us compare two systems: (i) the surface of a bulk magnetic medium with refractive index $n = n_B$, and (ii) a thin film of the same material on a substrate with $n = n_S$ and neglecting the SH contribution from the film-substrate interface. In the limits of vanishing film thickness and $\sin\theta \ll n$, applying Eqs. (3) and (5), and using the standard Fresnel reflection theory, one can easily show that for s-polarized input the ratio of the reflected SH fields due to the odd (E_s) and even (E_p) terms is given by

$$\frac{E_s(2\omega)}{E_p(2\omega)} \propto \frac{1 + R_s(2\omega)}{1 + R_p(2\omega)} = \frac{1}{n(2\omega)}, \tag{6}$$

with n equal to n_B or n_S. Similar relations hold for p-polarized input. Equation (6) shows that the multilayer SHG effects will be more pronounced for a thin film on a low refractive index substrate ($n_S \ll n_B$) than for a bulk material.

In conclusion, we have observed enhancements of almost 3 orders of magnitude for the nonlinear Kerr rotation relative to the linear one, for an Fe(2 nm)/Cr(2 nm) multilayer on a Si–silicon oxide substrate. The experimental results can easily be understood from the phenomenological approach by Pan, Wei, and Shen, if the proper local field factors are included. Contrary to the linear case, the surface sensitive nonlinear rotation is unaffected by the thickness reduction of the magnetic film. Scaling these results to the surface of a bulk Fe crystal gives good agreement with theoretical predictions, based on band structure calculations. It is shown that, by varying the angle of incidence, the nonlinear Kerr angle may be tuned at will between 0° and 90°. This may lead to interesting applications for imaging of magnetic domains, as large $\phi_K^{(2)}$ are obtained for very thin magnetic films that have vanishingly small linear Kerr rotation.

We would like to thank H. A. Wierenga and M. W. J. Prins for stimulating discussions. We thank M. A. C. Devillers for the ellipsometry measurements. Part of this work was supported by the Stichting Fundamenteel Onderzoek der Materie (FOM), which is financially supported by the Nederlandse Organisatie voor Wetenschappelijk Onderzoek (NWO).

[1] L. M. Falicov *et al.,* J. Math. Res. **5**, 1299 (1990), and references therein.

[2] A. Vaterlaus, M. Stampanoni, M. Aeschlimann, and F. Meier, J. Appl. Phys. **64**, 5331 (1988).

[3] C. L. Fu, A. J. Freeman, and O. Oguchi, Phys. Rev. Lett. **54**, 2700 (1985).

[4] A. Cebollada, R. Miranda, C. M. Schneider, P. Schuster, and J. Kirschner, J. Magn. Magn. Mater. **102**, 25 (1991).

[5] S. S. P. Parkin, N. More, and K. P. Roche, Phys. Rev. Lett. **64**, 2304 (1990).

[6] P. Bruno and C. Chappert, Phys. Rev. Lett. **67**, 1602 (1991); Phys. Rev. B **46**, 261 (1992).

[7] R. Coehoorn, Phys. Rev. B **44**, 9331 (1991).

[8] M. T. Johnsson *et al.,* Phys. Rev. Lett. **68**, 2688 (1992).

[9] U. Pustogowa, W. Hübner, and K. H. Bennemann, Phys. Rev. B **49**, 10 031 (1994).

[10] J. Reif, C. Rau, and E. Matthias, Phys. Rev. Lett. **71**, 1931 (1993).

[11] Y. R. Shen, *The Principle of Nonlinear Optics* (Wiley, New York, 1984).

[12] Ru-Pin Pan, H. D. Wei, and Y. R. Shen, Phys. Rev. B **39**, 1229 (1989).

[13] W. Hübner and K. H. Bennemann, Phys. Rev. B **40**, 5973 (1989).

[14] J. Reif, J. C. Zink, C. M. Schneider, and J. Kirschner, Phys. Rev. Lett. **67**, 2878 (1991).

[15] H. A. Wierenga, W. de Jong, M. W. J. Prins, Th. Rasing, R. Volmer, A. Kirilyuk, and J. Kirschner, Phys. Rev. Lett. **74**, 1462 (1995).

[16] G. Spierings, V. Koutsos, H. A. Wierenga, M. W. J. Prins, D. Abraham, and Th. Rasing, Surf. Sci. **287**, 747 (1993); J. Magn. Magn. Mater. **121**, 109 (1993).

[17] H. A. Wierenga, M. W. J. Prins, D. L. Abraham, and Th. Rasing, Phys. Rev. B **50**, 1282 (1994).

[18] Recently we have learned about the observation of a large $\phi_K^{(2)}$ for an oxidized Ni surface: K. Böhmer, J. Hohfeld, and E. Matthias (to be published).

[19] H. A. Wierenga, M. W. J. Prins, and Th. Rasing, Physica (Amsterdam) **204B**, 281 (1995).

[20] P. B. Johnson and R. W. Christy, Phys. Rev. B **9**, 5056 (1974); D. E. Aspnes and A. A. Studna, Phys. Rev. B **27**, 985 (1983).

[21] D. O. Smith, J. Appl. Phys. **36**, 1120 (1965).

[22] M. Groot Koerkamp and Th. Rasing (to be published).